Ion Solvation in Polarizable Chloroform: A Molecular Dynamics Study

Tsun-Mei Chang and Liem X. Dang*

Environmental Molecular Sciences Laboratory, Pacific Northwest National Laboratory, Richland, Washington 99352

Received: June 30, 1997; In Final Form: August 26, 1997[⊗]

The structural, thermodynamic, and dynamical properties of the alkali-metal cations and the halide anions in liquid chloroform are investigated using molecular dynamics simulation techniques. From the atomic radial distribution analysis, the chloroform molecules are found to form well-defined solvation shells around the alkali-metal cations and the halide anions. The size of the solvation cage and the coordination number both increase with increasing ion size. In liquid chloroform, all these ions are shown to induce a strong orientational order in the surrounding chloroform molecules as evidenced by the angular distribution functions. We found that the mean electric potentials induced by the chloroform molecules shifted to smaller magnitudes with increasing ion size. Because of the greater electric polarizabilities of the larger ions, the average induced dipole moments were enhanced with increasing ion size. The diffusion coefficients of the alkali-metal cations and the halide anions in liquid chloroform are estimated from the mean-square displacements and the velocity autocorrelation functions. Generally, the diffusion constants of the cations are larger than those of the anions. For the cations, the diffusion constants are of similar magnitudes and do not depend on the ion size. However, the diffusion coefficients of the halide anions show a strong dependence on the ion size. The motion of the first coordination shell chloroform molecules is examined via their velocity autocorrelation functions. These correlation functions behave very similarly, suggesting that the motion of the first solvation shell is not governed by the sizes or the charges of these ions. In addition, the residence time autocorrelation functions of the first solvation shell are evaluated. As expected, the residence time decreases as the ion size increases.

I. Introduction

Many of the theoretical and computational studies previously published have focused on the molecular properties of solutes in aqueous solutions.[1−7] Rather limited attention has focused on the ion solvation in nonaqueous solutions[8−10] despite the fact that many chemical and physical processes occur in organic solvents. This work describes a molecular dynamics investigation of the detailed solvation properties of alkali metal cations (Na^+, K^+, and Cs^+) and halide anions (F^-, Cl^- and I^-) in liquid chloroform and compares the results to those of the corresponding ionic water solutions. Chloroform is a good representative of apolar organic solvents that are used in ion extraction experiments, but to our knowledge it has not been used so far for simulations of ion solvation systems.[11] In addition, chloroform was widely used in the processing of radioactive materials and contributes significantly to nuclear waste problems.[12] By characterizing the solvation properties and the molecular interactions of these ion−chloroform solutions, it will enable us to better understand these environmental issues and help us control chemical processes in liquid chloroform. The simulations described in this paper differ from most previous studies of ion solvation by explicitly including the molecular polarizability for both solvent and solute molecules. Due to the strong local electrostatic fields induced by the highly charged ions in these systems, an explicit treatment of the polarizability provides a more realistic description of the solvation properties of the ion−chloroform solutions.

In section II, we briefly describe the polarizable model potentials used in this study and the computational details of the molecular dynamics (MD) simulations. The solvation structures and the thermodynamic properties of alkali-metal cations and halide anions in liquid chloroform are discussed in section III. The results of the electrostatic properties of the ions are presented in section IV. In section V, the dynamical properties of the ions and their first solvation shell chloroform molecules are discussed. Comparisons of these computed properties to the available results of aqueous ionic solutions are also made. The conclusions are presented in section VI.

II. Potential Model and Computational Details

In this study, a rigid all-atom nonadditive polarizable potential model is adapted to describe the chloroform intermolecular interactions. Each chloroform molecule is fixed at the experimental geometry with the C−Cl and C−H bond lengths of 1.76 and 1.07 Å, and Cl−C−Cl and Cl−C−H bond angles of 111.2° and 107.6°, respectively. In this model, fixed atomic charges, Lennard-Jones potential parameters, and point polarizability are assigned to each atom in chloroform to describe the Coulombic, the van der Waals, and the nonadditive polarization interactions. This polarizable chloroform potential was developed to accurately reproduce the thermodynamic and dynamical properties of the liquid and the liquid/vapor interface of chloroform.[11] The ion parameters are taken from the literature and were obtained by fitting to the gas-phase incremental binding enthalpies for small ion−water clusters.[7,14−16] The potential parameters used in this study are summarized in Table 1.

The total interaction energy of the ion-chloroform system can then be written as

$$U_{\text{tot}} = U_{\text{pair}} + U_{\text{pol}} \tag{1}$$

$$U_{\text{pair}} = \sum_i \sum_j \left(4\epsilon \left[\left(\frac{\sigma_{\text{ij}}}{r_{ij}} \right)^{12} - \left(\frac{\sigma_{ij}}{r_{ij}} \right)^{6} \right] + \frac{q_i q_j}{r_{ij}} \right) \tag{2}$$

and

[⊗] Abstract published in *Advance ACS Abstracts,* November 15, 1997.

S1089-5647(97)02101-9 CCC: $14.00

TABLE 1: Potential Parameters for Chloroform, Halide Anions, and Alkali-Metal Cations Used in the Molecular Dynamics Simulations[c]

atom type	σ (Å)	ϵ (kcal/mol)	q (e)	α (Å^3)
C	3.410	0.137	0.5609	0.878[a]
Cl	3.450	0.275	−0.1686	1.910[a]
H	2.810	0.020	−0.0551	0.135[a]
Na^+	2.350	0.130	1.0000	0.240[b]
K^+	3.154	0.100	1.0000	0.830[b]
Cs^+	3.831	0.100	1.0000	2.440[b]
F^-	3.359	0.100	−1.0000	1.050[b]
Cl^-	4.450	0.100	−1.0000	3.250[b]
I^-	5.167	0.100	−1.0000	6.902[b]

[a] Applequist, J.; Carl, J. R.; Fung, K.−K. *J. Am. Chem. Soc.* **1972**, *94*, 2952. [b] Pauling, L. Proc. R. Soc. London, *Ser. A* **1927**, *114*, 191. [c] σ and ϵ are the Lennard-Jones parameters, q is the atomic charge, and α is the atomic polarizability.

$$U_{\text{pol}} = -\sum_{i=1}^{N} \mu_i \cdot E_i^0 - \frac{1}{2}\sum_{i=1}^{N}\sum_{j=1,i\neq j}^{N} \mu_i \cdot T_{ij} \cdot \mu_j + \sum_{i=1}^{N} \frac{|\mu_i|^2}{2\alpha_i} \quad (3)$$

Here, r_{ij} is the distance between site i and j, q is the charge, and σ and ϵ are the Lennard-Jones parameters. E_i^0 is the electric field at site i produced by the fixed charges in the system, μ_i is the induced dipole moment at atom site i. The first term in eq 3 represents the charge-dipole interaction, the second term describes the dipole−dipole interaction, and the last term is the energy associated with the generation of the dipole moment μ_i. During the molecular dynamics simulations, a standard iterative self-consistent-field procedure is used to evaluate the induced dipoles.

The molecular dynamics simulations were performed on a ion−chloroform system containing 265 chloroform molecules and a single ion (Na^+, K^+, Cs^+, F^-, Cl^-, and I^-) in a cubic simulation cell with linear dimension roughly equal to 31 Å. The simulations were carried out in an isobaric−isothermal ensemble at 1 atm and 298 K, with periodic boundary condition applied in all three spatial dimensions. A coupling constant of 0.2 ps is used for the pressure relaxation. The temperature of the system is maintained at 298 K by coupling to a external thermal bath with a time constant of 0.1 ps. The velocities generated from a Maxwell−Boltzmann distribution at 298 K was assigned to each atom initially. During the entire simulation, the internal geometry of every chloroform molecule is fixed by constraining its bond lengths via the SHAKE algorithm,[17] and a time step of 2 fs is used to solve the equations of motion. The interactions are truncated at a molecular center-of-mass separation of 15 Å. For each ion, a 100-ps trajectory is carried out to equilibrate the ion−chloroform system, followed by at least 200-ps of data collection for analysis.

III. Thermodynamic and Structural Properties

In this section, the results of the solvation energies and structures of the alkali metal cations and halide anions in liquid chloroform are presented. Details of the solvation structures are obtained by examining the atomic radial distribution functions and the angular probability distributions. These analyses reveal the local structures of solvent molecules around the ions as well as the orientations of the solvent molecules with respect to the ions.

The solvation energy of an ion in liquid chloroform is calculated as the difference between the total potential energy of the ion−chloroform solution and a pure liquid chloroform system. A summary of the solvation energies of alkali-metal cations and halide anions in liquid chloroform at 298 K and 1 atm is shown in Table 2. Clearly and as expected, the solvation energy decreases with increasing ion size. In general, these solvation energies are smaller than the corresponding values for the ions in water because of the weaker ion−chloroform intermolecular interactions. No experimental data were found for the solvation energies in chloroform. For the case of Cs^+ in chloroform, the solvation energy is estimated to be −41.9 kcal/mol, which is slightly stronger than −36.5 kcal/mol determined for Cs^+ in liquid carbon tetrachloride.[18] This result may be attributed to the favorable electrostatic interactions between the ions and the permanent dipole moments of the chloroform molecules.

TABLE 2: Solvation Energy, Average Coordination Number of the Alkali-Metal Cations, and Halide Anions in Liquid Chloroform at 298 K from the Molecular Dynamics Simulations

ion	solvation energy (kcal/mol)	coordination number	$g_{IC}(r)$ first minima
Na^+	−70.5 ± 3.1	6.0	5.25
K^+	−59.5 ± 2.8	7.9	5.65
Cs^+	−50.8 ± 2.5	9.5	6.00
F^-	−72.8 ± 3.0	5.9	4.60
Cl^-	−56.5 ± 2.1	7.8	5.05
I^-	−51.5 ± 2.1	9.1	5.60

The ion−carbon, ion−chlorine, and ion−hydrogen atomic radial distribution functions are depicted in Figure 1a−c for alkali-metal cations and Figure 2a−c for halide anions. Clearly, there are distinctive features in these pair correlation functions, indicating the presence of a local structural order of chloroform molecules around these ions. In addition, we observe well-characterized first peaks in the ion−carbon, site−site distribution functions. This result suggests that chloroform molecules form a well-defined first solvation shell around the ions. At larger ion−carbon separations, weak second peaks are also observed, indicating a less tight second solvation shell. The running numbers of the chloroform molecules in the first solvation shell of the ion can be evaluated by integrating the ion−carbon radial distribution functions to the first minimum. The results are listed in Table 2. It is clear that as the ion size increases, the coordination number increases. Accompanying the increase in the coordination number, we observe that the first peaks become broader and shift to larger ion−carbon separations, indicating an increase of the solvation cage size and a weakening of the cation−chloroform interactions.

For the three alkali metal cations, we consistently find that the first peak positions occur at small, intermediate, and large distances for the cation−chlorine, cation−carbon, and cation−hydrogen radial distribution functions, respectively. These features imply the chloroform molecules in the first solvation shell are oriented in such a way that all three chlorine atoms are facing the ion with the hydrogen atoms pointing the opposite direction. This specific configuration is energetically preferable by maximizing the attractive Coulombic interactions between the cations and the negatively charged chlorine atoms. Detailed examination of the ion−chloroform orientation will be further discussed in the next section.

Interestingly, the situation is reversed for the anions. The first peaks of the anion-chlorine, anion-carbon, and anion-hydrogen radial distribution functions appear at the longest, intermediate, and shortest distances as illustrated in Figure 2a−c. These results correspond to an orientation in which the hydrogen atom is pointing toward the anion and the chlorine atoms are pointing away from the anion in the first solvation shell. This result can be explained in terms of an energetic consideration. By having the hydrogen atom facing the anions,

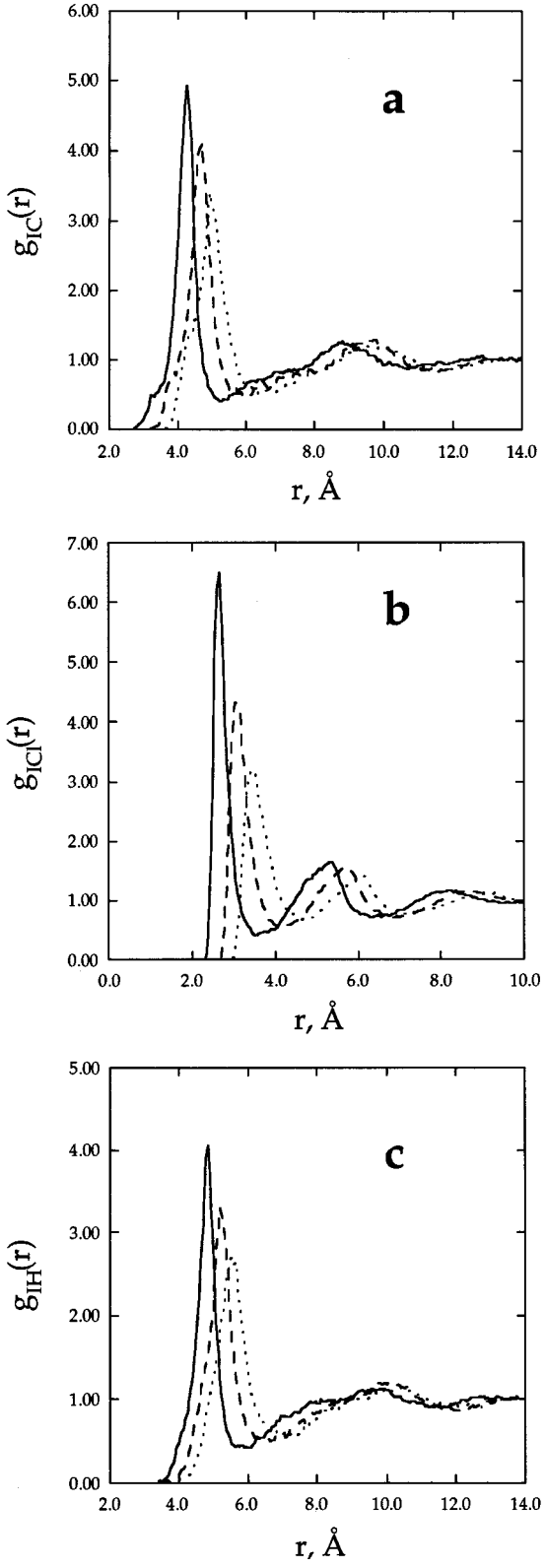

Figure 1. Computed (a) ion−carbon, (b) ion−chlorine, and (c) ion−hydrogen atomic radial distribution functions for a single Na^+ (solid), K^+ (dashed), and Cs^+ (dotted) cation in liquid chloroform at 298 K, respectively.

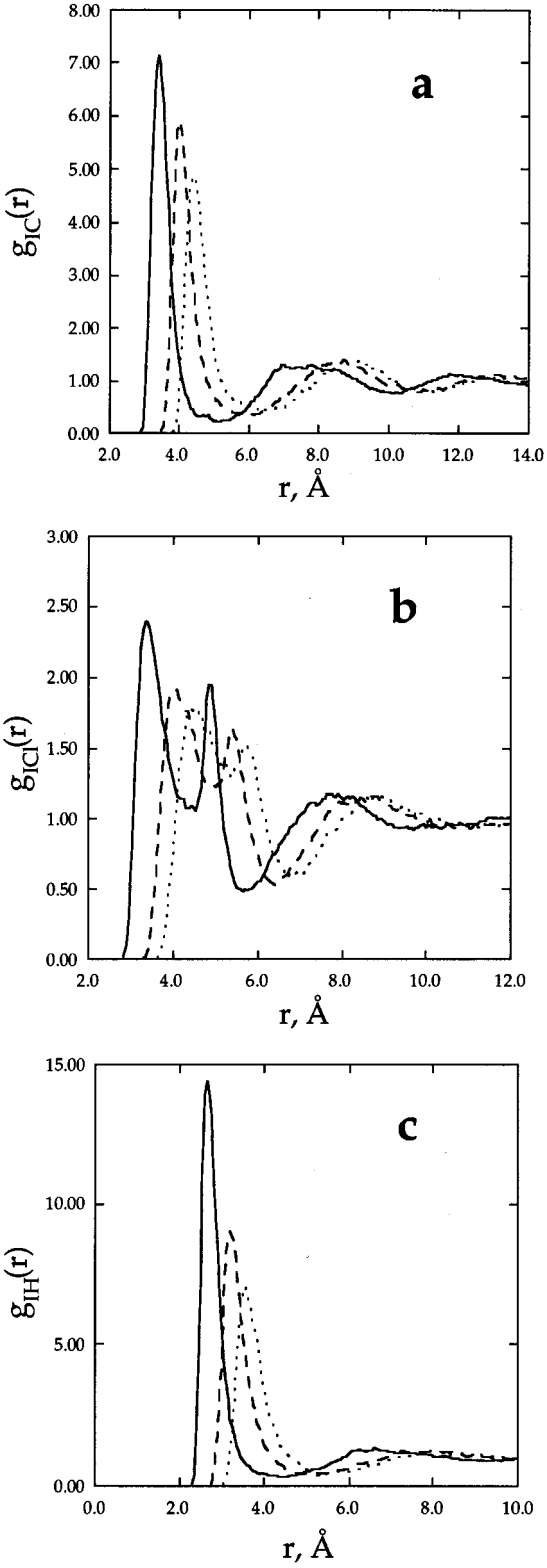

Figure 2. Computed (a) ion−carbon, (b) ion−chlorine, and (c) ion−hydrogen atomic radial distribution functions for a single F^- (solid), Cl^- (dashed), and I^- (dotted) anion in liquid chloroform at 298 K, respectively.

the unfavorable repulsive electrostatic interactions were minimized between large negatively charged chlorine atoms and anions.

By analyzing the angular distribution functions as a function of the ion−carbon distance, the local orientation of the chloroform molecules with respect to the ions can be examined. Representative angular distribution functions between chloroform molecules and the alkali metal cations and the halide anions, respectively, are shown in Figures 3 and 4. In Figure 3a,b, two angular distribution functions are shown describing the orientation between the chloroform molecules and K^+ as a function of chloroform−K^+ separation. The probability distribution of the angle between the intramolecular C−Cl bond and C−K^+ vector as a function of C−K^+ distance is shown in Figure 3a. The angle in Figure 3b is defined between the

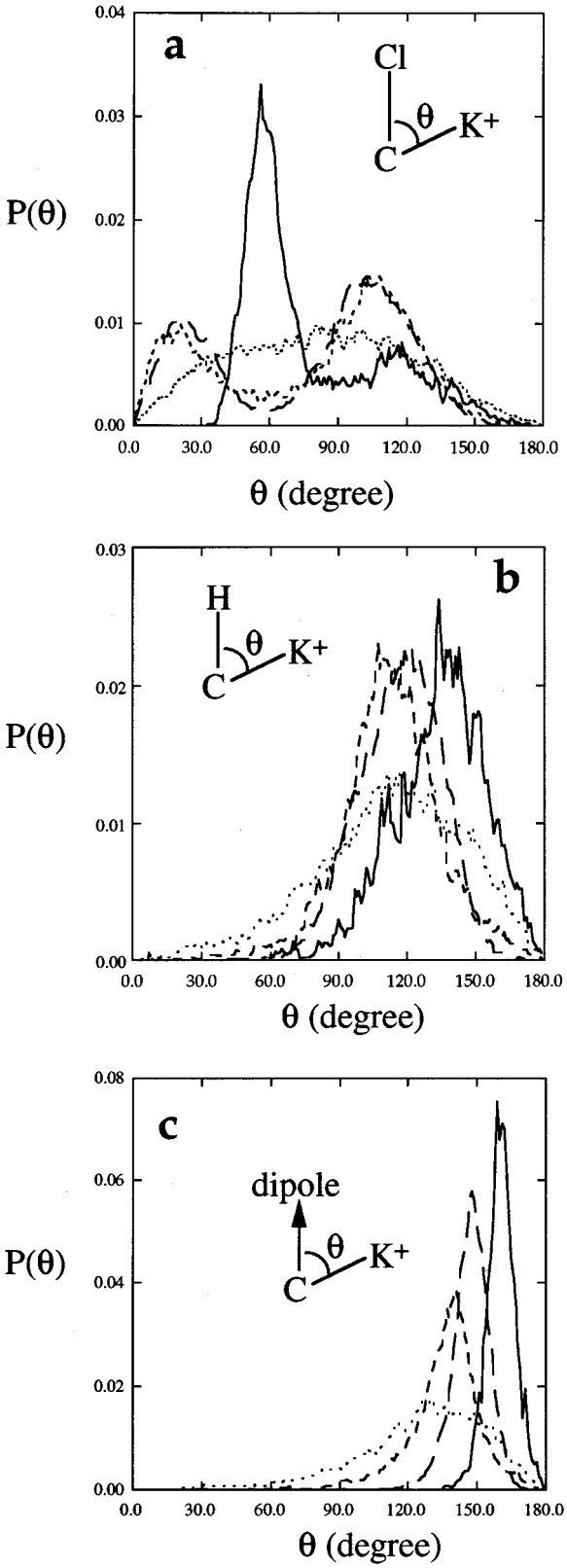

Figure 3. Angular distribution functions between the K^+ ion and the surrounding chloroform molecules as a function of the C−K^+ distance. The angle is defined between the C−K^+ vector and (a) the intramolecular C−Cl bond, (b) the intramolecular C−H bond, and (c) the dipole moments of the chloroform molecules. The data points correspond to C−K^+ distances 0−4 (solid), 4−5 (long dashed), 5−6 (short dashed), and 6−7 Å (dotted), respectively.

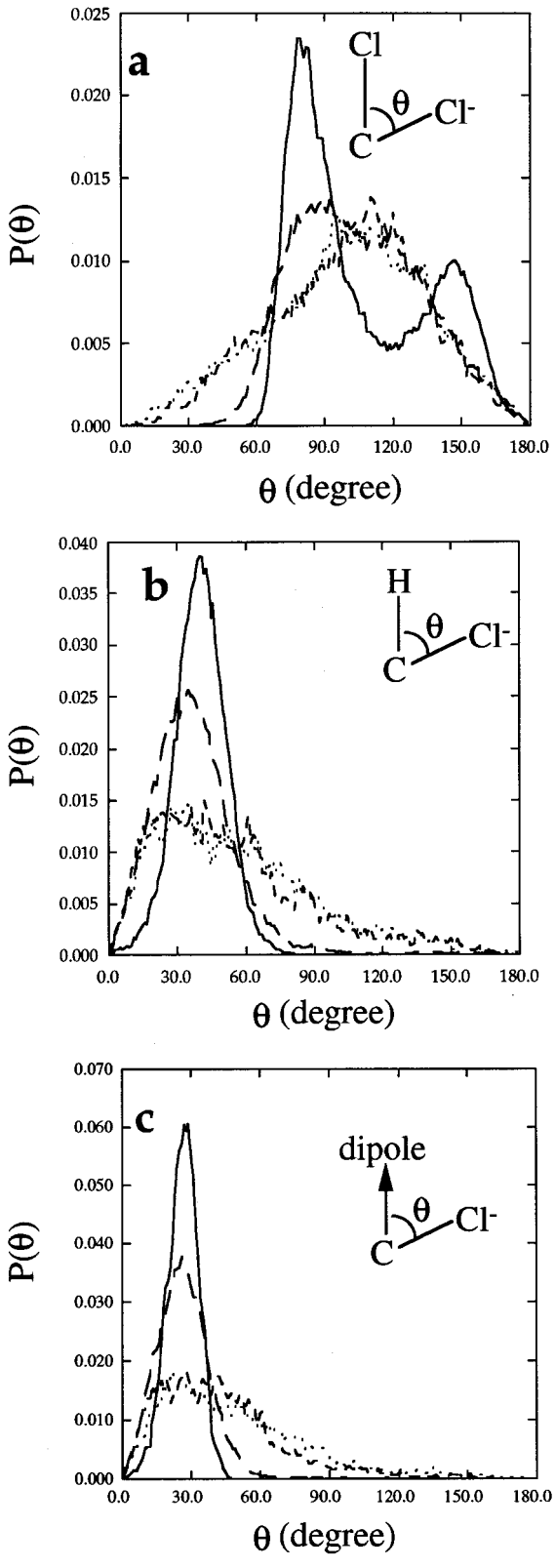

Figure 4. Angular distribution functions between the Cl^- ion and the surrounding chloroform molecules as a function of the C−Cl^- distance. The angle is defined between the C−Cl^- vector and (a) the intramolecular C−Cl bond, (b) the intramolecular C−H bond, and (c) the dipole moments of the chloroform molecules. The data points correspond to C−Cl^- distances 0−4 (solid), 4−5 (long dashed), 5−6 (short dashed), and 6−7 Å (dotted), respectively.

intramolecular C−H bond and the C−K^+ vector. When the C−K^+ distance is less than the first minimum position in the $g_{CK}(r)$, the probability distributions show significant deviations from the sine function that describes an uniform orientation. Interestingly, for the chloroform molecules residing inside a sphere of 4 Å around the K^+ ion, a major peak centered at 56° appears in Figure 3a and a main peak centered at 139° appears in Figure 3b. This result implies that all of the three chlorine

atoms are facing K^+ with the hydrogen atom pointing outward. This specific configuration is probably caused by the competition between the electrostatic interactions that favors a situation in which the chlorine atoms point directly toward K^+ and the steric effect that avoids the close contact between the chlorine atoms and the K^+ ion. As the $C-K^+$ distance increases, it is found that the peak positions shift to 21° and 102° in Figure 3a, and to 121° in Figure 3b. This result corresponds to a situation in which only one of the chlorine atoms is pointing toward the potassium ion and the other two chlorine atoms and the hydrogen atom are pointing away from the potassium ion. This orientation can be attributed to the favorable electrostatic interactions. These results clearly suggest that the potassium ion induces a strong orientational order in liquid chloroform. As the $C-K^+$ distance increases further, we observe that the angular probability distribution approaches the sine function, indicating a decrease in the structural order. However, even at the $C-K^+$ separation of 8 Å, there is still a persistent orientational order between the chloroform molecules and K^+, as clearly indicated by the angular distribution function between the C−H bond and the $C-K^+$ vector in Figure 3b.

In Figure 3c, the probability distributions of the angle between the dipole moment vectors of the chloroform molecules and the $C-K^+$ vector is depicted as a function of the $C-K^+$ distance. A major peak is centered at 160° for small $C-K^+$ separation, indicating that the dipole moments of chloroform are pointing away from the potassium ion. This conclusion is consistent with the results from Figure 3a,b and is attributed to the favorable electrostatic interactions. As the $C-K^+$ distance increases, the orientational order decreases. Interestingly, the dipole moment vectors still show preferred orientations with respect to K^+ at larger separations. The same trend is also observed for Na^+ and Cs^+ in liquid chloroform, although data are not shown.

The angular distribution functions between the chloroform molecules and the Cl^- ion are shown in Figure 4a−c. The angles are defined between the $C-Cl^-$ vector with respect to the intramolecular C−Cl bond, C−H bond, and the dipole moment, respectively. As expected, it is observed that the orientation between the chloroform molecules and the halide anions behaves in a way that is significantly different from that between the chloroform molecules and the cations. For a $C-Cl^-$ separation less than 4 Å, two major peaks centered at 79° and 147° appear in Figure 4a and a major peak centered at 40° is observed in Figure 4b. These results clearly indicate that the hydrogen atom and two chlorine atoms are pointing to the Cl^- ion, with one of the chlorine atoms extending away from the Cl^- ion as a result of balancing the electrostatic interactions and the steric effect. At slightly larger $C-Cl^-$ distances, the electrostatic interactions dominate, leading to the shift of the peak position to a smaller angle in Figure 4b. At the same $C-Cl^-$ separation, the two main peaks merge into one peak centered around 89° in Figure 4a. This suggests that the C−H bond is nearly pointed directly at the Cl^- ion, and the C−Cl bonds are pointed away from the Cl^- ion, which is energetically preferred by the electrostatic attractions. For longer $C-Cl^-$ distances, the angular distribution functions are found to approach normal sine distributions, implying a decrease in the local orientational order. The difference in the orientation of chloroform molecules around anions with respect to cations is also revealed by examining the angular probability distributions between the dipole moments of $CHCl_3$ and the $C-Cl^-$ vector as shown in Figure 4c. Note that the main peak is centered at 30−40°, which is significantly different from the case of cations where the peak is centered around 160°. This observation suggests that the dipole moments of chloroform are pointing to the anions but pointing away from cations as expected. Interestingly, the orientational order between ions and dipole moments of chloroform molecules persists even at larger distances. In a MD study of Na^+ and Cl^- ion in water,[7] Smith and Dang also observed a similar behavior that the dipole moments of water are directed toward the anions and pointing away from the cations.

IV. Electrostatic Properties

With the use of polarizable interaction potentials, we are able to describe the molecular electrostatic properties more realistically. For example, it allows us to describe the induced polarization effects of ions in liquid chloroform while no induced dipole moments can be accounted for with the nonpolarizable potentials. In the following section, the electrostatic properties of the alkali metal cations and halide anions in liquid chloroform are characterized via the electrostatic potential distributions at the ion positions and the induced dipole moment distributions of the ions in liquid chloroform.

Depicted in Figure 5a are the distribution functions of the electric potentials experienced by the Na^+, K^+, and Cs^+ cations that are induced by the surrounding chloroform molecules. Obviously, the electric potential distributions are not symmetric and cannot be described as Gaussian distributions. It is clear from Figure 5a that the average electric potential shifts to a larger magnitude as the ion size decreases. This result may be due to the more tightly held solvation shells for smaller ions. The much closer chloroform molecules thus induce stronger electric potentials at the ion locations. The probability distributions of the electric potentials at the F^-, Cl^-, and I^- ion locations are shown in Figure 5b. First, we notice that the sign of the electric potentials have been altered from the case of the cations to that of the anions. This result indicates a change of the orientation of the chloroform molecules around the ions. It is also observed that the electric potential distributions center at larger magnitudes for smaller anions, which may be induced by the chloroform molecules in the more tightly bound solvation shells.

Because of the presence of the local electric fields induced by the neighbor chloroform molecules, the ions become polarized and possess induced dipole moments. Shown in parts a and b of Figure 6 are the probability distribution functions for the induced dipole moments of alkali metal cations (Na^+, K^+, and Cs^+) and halide anions (F^-, Cl^-, and I^-) in liquid chloroform, respectively. Obviously, the induced dipole moment distributions become much broader with the increasing ion sizes. As expected, the average induced dipole moment of the ions increases as the size of the ions increases, possibly due to the greater polarizability of the larger ions.

V. Dynamical Properties

By analyzing the diffusion coefficients, the velocity autocorrelation functions, and the residence time correlation functions, the motion of the ions relative to the solvating chloroform molecules are investigated.

From molecular dynamics simulations, the diffusion constants of the alkali metal cations and halide anions in liquid chloroform can be conveniently evaluated from the velocity autocorrelation function, $\hat{C}_{vv}(t)$[19]

$$\hat{C}_{vv}(\tau) = \langle V(0)\cdot V(\tau)\rangle = \frac{1}{t_{\max}}\sum_{t=0}^{t_{\max}} V(t+\tau)\cdot V(t) \qquad (4)$$

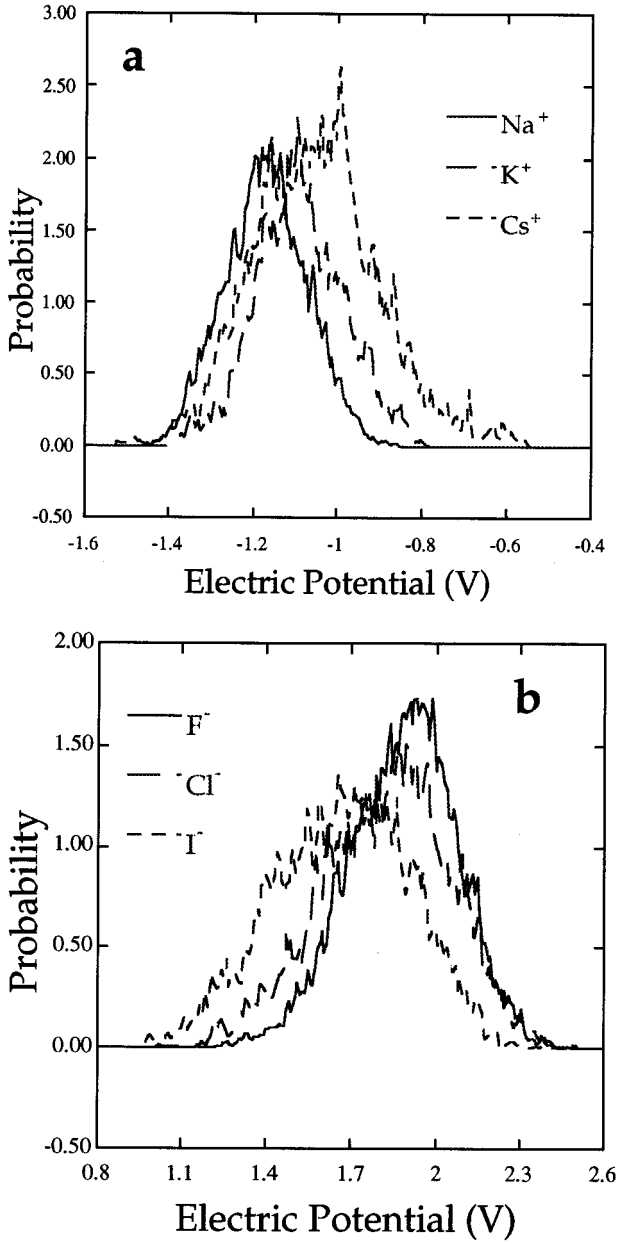

Figure 5. Distribution functions of the electric potentials at the ion positions induced by the surrounding chloroform molecules from molecular dynamics simulations of (a) alkali-metal cations (Na^+, K^+, Cs^+) and (b) halide anions (F^-, Cl^-, I^-) in liquid chloroform at 298 K.

Here, $V(t)$ is the velocity of the ion at time t and t_{max} is the total number of time steps. The velocity autocorrelation function is usually normalized by

$$C_{vv}(\tau) = \frac{\langle V(0)\cdot V(\tau)\rangle}{\langle V(0)\cdot V(0)\rangle} \tag{5}$$

In Figure 7a,b, we show the normalized velocity autocorrelation functions for the cations, Na^+, K^+, and Cs^+ and the anions, F^-, Cl^-, and I^- in liquid chloroform as a function of time. The computed velocity autocorrelation functions show a fast initial decay followed by some oscillations. This oscillatory behavior of $C_{vv}(t)$ may come from the rattling motion of the solute ion inside the first solvation shell of $CHCl_3$. Interestingly, the velocity autocorrelation function shows more pronounced oscillations for smaller ions and less oscillations for ions with increasing sizes. This result is expected because that the first solvation shells becomes more diffused and less tightly held as the ion size increases. According to the Green−Kubo relation,[20]

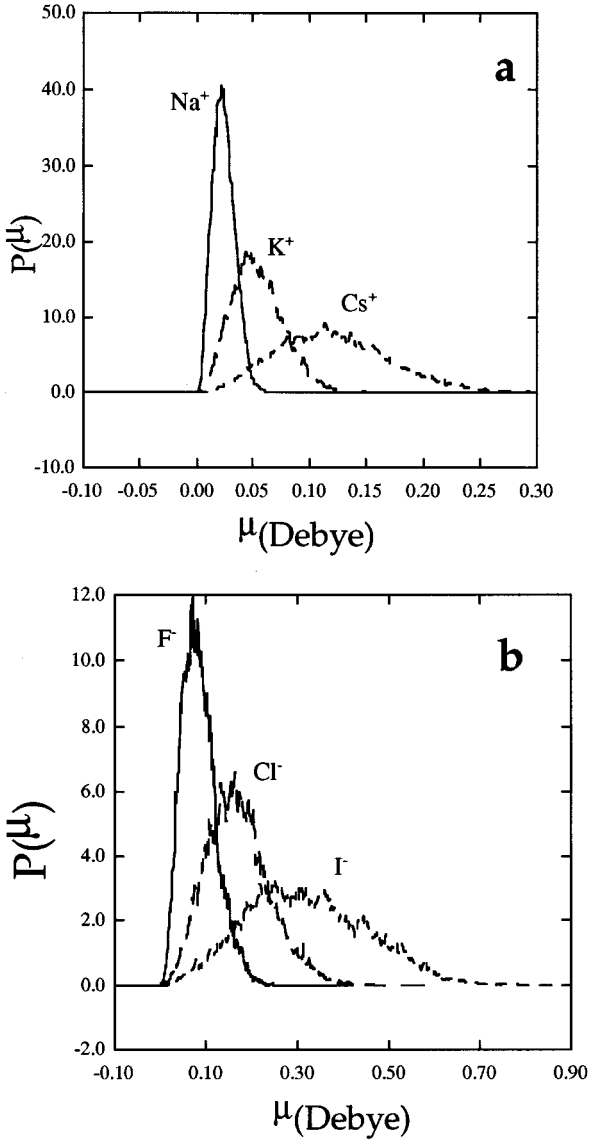

Figure 6. Computed induced dipole moment distributions of (a) the alkali-metal cations (Na^+, K^+, and Cs^+) and (b) the halide anions (F^-, Cl^-, and I^-) in liquid chloroform at 298 K.

the diffusion coefficient can be determined by integrating the velocity autocorrelation function

$$D = \frac{1}{3}\lim_{t\to\infty}\int_0^t \hat{C}_{vv}(t)\,dt \tag{6}$$

The computed diffusion constants from the velocity autocorrelation functions are summarized in Table 3.

Another independent method of evaluating the diffusion coefficients from the mean-square displacement of the ions in liquid chloroform is via the well-known relation

$$D = \frac{1}{6}\lim_{t\to\infty}\frac{d}{dt}\langle |r(t) - r(0)|^2\rangle \tag{7}$$

where $r(t)$ represents the coordinates of the ion at time t. The calculated ion mean square displacements at 298 K are displayed in parts and b of Figure 8 as a function of time for cations and anions, respectively. The diffusion coefficients are determined from the least-squares fits to the mean-square displacements and are summarized in Table 3.

In general, the diffusion coefficients estimated from the mean-square displacements are in reasonable agreement with those determined from the velocity autocorrelation functions. Inter-

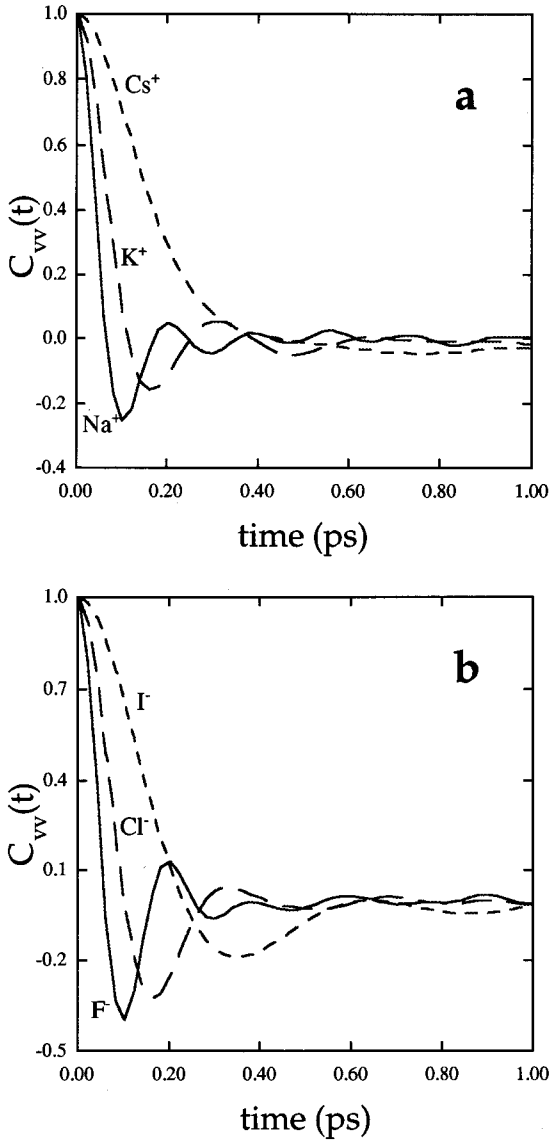

Figure 7. Normalized velocity autocorrelation functions of (a) the alkali-metal cations (Na^+, K^+, Cs^+) and (b) the halide anions (F^-, Cl^-, I^-) in liquid chloroform from the molecular dynamics simulations at 298 K.

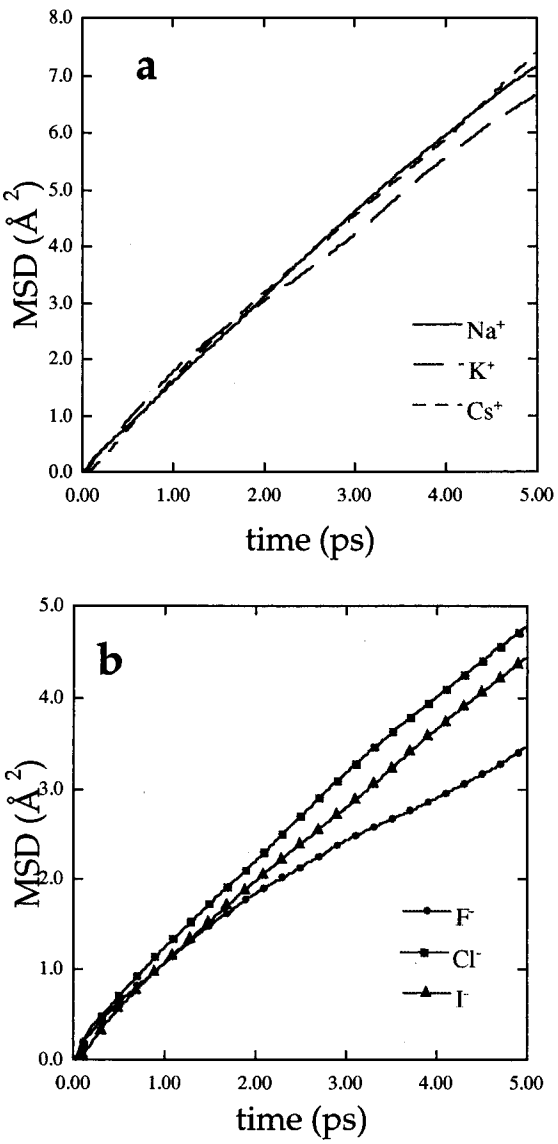

Figure 8. Mean-square displacements of (a) the alkali-metal cations (Na^+, K^+, Cs^+) and (b) the halide anions (F^-, Cl^-, I^-) in liquid chloroform from the simulations at 298 K.

TABLE 3: Diffusion Coefficients (10^{-5} cm^2/S) of Alkali Metal-Cations and Halide Anions in Liquid Chloroform at 298 K Calculated from the Velocity Autocorrelation Functions (VAF) and the Mean-Square Displacements (MSD) and the Residence Time of Chloroform Molecules in the First Solvation Shell

			residence time (ps)	
ion	VAF	MSD	chloroform	water[a]
Na^+	1.96 ± 0.21	2.30 ± 0.22	34.7	15.0
K^+	1.97 ± 0.23	2.06 ± 0.24	30.8	4.8
Cs^+	2.28 ± 0.23	2.33 ± 0.23	31.9	5.0
F^-	0.53 ± 0.04	0.86 ± 0.05	125.4	20.0
Cl^-	1.16 ± 0.07	1.42 ± 0.07	38.9	5.0
I^-	1.29 ± 0.08	1.40 ± 0.06	46.9	2.5

[a] Reference 19.

estingly, the diffusion constants show a strong dependence on the ion charges. For all three cations, we found similar diffusion coefficients regardless of its size. The diffusion coefficients of halide anions are much smaller compared to those of alkali-metal cations, implying that the halide anions travel much more slowly than the alkali metal cations in liquid chloroform. Additionally, we observe that the diffusion constants increase significantly as the size of anion increases. The decreasing ion−chloroform interactions may be responsible for this behavior. The extremely small diffusion coefficient of the F^- ion may also be caused by the strong ion−solvent cage interactions as indicated by the very long residence time of the first solvation shell chloroform molecules as will be discussed in a later section.

In addition to the ion velocity autocorrelation functions, we calculate the center-of-mass velocity correlation functions of the first coordinate shell chloroform molecules to examine the motion of the solvation shell. This autocorrelation function is defined as[1]

$$C_{ss}(t) = \frac{\langle V_s(0) \cdot V_s(t) \rangle}{\langle V_s(0) \cdot V_s(0) \rangle} \tag{8}$$

In eq 8, $V_s(t)$ is the sum of the center of mass velocity of the chloroform molecules that reside inside the first solvation shell, which is defined by the first minimum in the ion−carbon radial distribution functions. The velocity correlation functions of the first solvation shell chloroform molecules are depicted in Figure 9a for the cations and in Figure 9b for the anions. We notice first that these velocity autocorrelation functions decay to zero on the same time scale and behave very similarly for all the

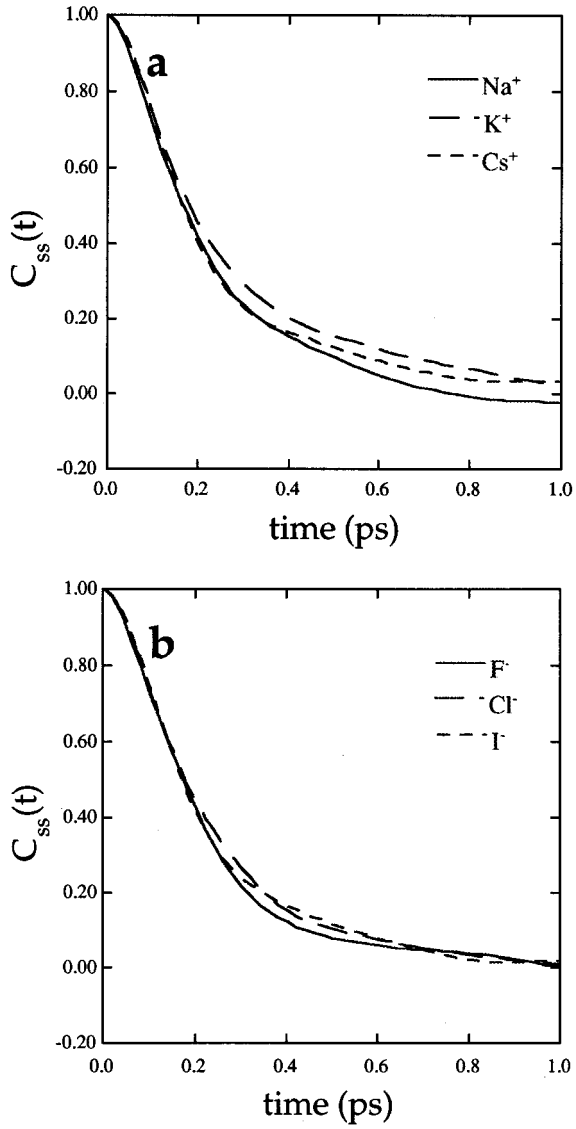

Figure 9. Velocity autocorrelation functions of the first solvation shell chloroform molecules for (a) the alkali-metal cations (Na^+, K^+, Cs^+) and (b) the halide anions (F^-, Cl^-, I^-) in liquid chloroform from the molecular dynamics simulations at 298 K.

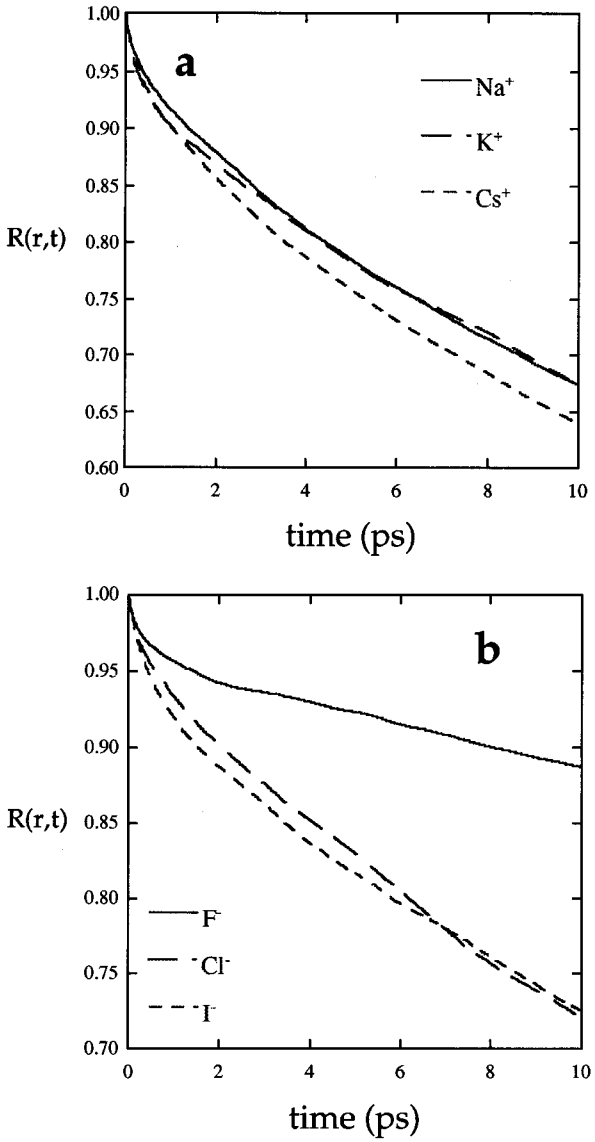

Figure 10. Residence time autocorrelation function for the first solvation shell chloroform molecules around (a) the alkali metal cations and (b) the halide anions.

ions investigated. This result suggests that the motion of the first solvation shell is not influenced nor hindered by the sizes or the charges of the ions.

It is also noted that the first coordination shell velocity correlation functions decay on a longer time scale compared to that of the ion velocity correlation functions regardless of their sizes or charges. This conclusion is significantly different from the case of the ion−water solutions, where the hydration shell velocity autocorrelation functions of water molecules decay more slowly for small cations but are more strongly damped for anions and larger cations. Oscillations are also observed in these hydration shell velocity autocorrelation functions.[1,2] This result was attributed to the fact that the first hydration shells of the smaller cations disrupted the hydrogen bonding network in liquid water. For liquids with no specific directional bonding and rather weak intermolecular interactions such as liquid chloroform, the velocity autocorrelation functions are expected to behave in a similar fashion as the case of the smaller cations in water, as clearly observed in Figure 9a,b.

To further characterize the motion of the first solvation shell relative to the ion, it is useful to calculate the residence time correlation function defined as[4,5,21]

$$R(r,t) = \frac{1}{N_r}\sum_{i=1}^{N_r}[\theta(r,0)\,\theta(r,t)] \qquad (9)$$

In eq 9, $\theta(r,t)$ is the Heaviside step function. It equals 1 when the chloroform molecule i stays inside the first coordination shell and 0 when the chloroform molecule leaves the first solvation shell. N_r is simply the average number of the chloroform molecules in the first solvation shell (coordination number) and t is the time. The residence time correlation function provides a rough estimate of the time period that a given solvent molecule spends inside the first coordination shell of the ion and is clearly dependent on the strength of the intermolecular interactions between the ion and the solvent molecules. The residence correlation functions as a function of time are displayed in Figure 10a for cations and in Figure 10b for anions. Except for a very short time, the correlation functions are well described by a single-exponential decay. Thus, the residence time of the first solvation shell chloroform molecules can be determined by fitting the correlation functions to an exponential decay function. The decay times are summarized in Table 3.

The results listed in Table 3 indicate that the residence time

is larger for the smaller ions. We also observed that the residence time correlation functions decay much more slowly for anions than for cations. Previous theoretical studies have suggested that the molecular reorientation is responsible for the breakup of the first solvation shell.[1,22] Therefore, this result may be due to the distinct orientational order between the chloroform molecules in the first solvation shell with respect to cations versus anions. Interestingly, the decay time of the first coordination shell solvent molecules is found to be much longer for the ion−chloroform solutions than that of the ion−water systems. This phenomenon may be caused by the steric effect because it is easier for a rather small molecule like water to move than for a much bigger molecule like chloroform to move in a condensed-phase environment.

VI. Conclusion

We carried out a series of classical molecular dynamics simulations to examine the thermodynamic, structural, electrostatic, and dynamical properties of alkali-metal cations and halide anions in liquid chloroform. These simulations were performed at 298 K and 1 atm, and many-body polarizable model potentials were used to describe the molecular interactions.

From the atomic pair correlation function analyses, it is found that the chloroform molecules form well-defined solvation shells around the alkali metal cations and halide anions. The size of the solvation shell and the coordination number both increases as the ion size increases. In bulk liquid chloroform, all these ions are shown to induce a strong local orientational order in the neighbor chloroform molecules as evidenced by the angular distribution functions. In addition, the surrounding chloroform molecules show distinct orientations with respect to cations verse anions. Similar behavior is also observed in the ion−water systems.

With the use of the many-body polarizable potentials, the electrostatic properties of the ions in liquid chloroform can be more realistically modeled. It is found that the mean electric potentials induced by the chloroform molecules shift to smaller magnitudes with the increasing ion size. As the ion size increases, the average induced dipole moments are enhanced because of their greater electric polarizabilities.

To examine the dynamical properties of the ions in liquid chloroform, the diffusion coefficients of the alkali-metal cations and halide anions are estimated from the mean-square displacements and the velocity autocorrelation functions. Interestingly, the trend of the diffusion coefficients strongly depend on the ion charges. It is observed that diffusion constants of the cations are greater than those of the anions. For the alkali metal cations, the diffusion constants are of a similar magnitude. However, we found a strong dependence of the diffusion coefficients on the ion size for the halide anions. The motion of the first solvation shell chloroform molecules are examined via the velocity autocorrelation functions. These correlation functions behave very similarly, suggesting that the motion of the first solvation shell is not influenced nor hindered by the sizes or the charges of the ions. Interestingly, the first coordination shell velocity function of $CHCl_3$ is found to decay more slowly that the ion velocity function independent of the ion size or charges. This result is very different from the ion−water systems, where the hydration shell velocity correlation functions show pronounced dependence on the ion size or charges. The discrepancy can be traced back to the nature of ion−solvent interactions. In addition, we calculated the residence time autocorrelation functions of the first solvation shell chloroform molecules, which yields an estimate of the time scale for a solvent molecule residing in the first solvation shell. It is observed that the residence solvation time decreases as the ion size increases.

Acknowledgment. This work was performed at Pacific Northwest National Laboratory under the auspices of the Division of Chemical Sciences, Office of Basic Energy Sciences, U.S. Department of Energy. Battelle Memorial Institute operates the Pacific Northwest National Laboratory for the Department of Energy. Computer resources were provided by the Division of Chemical Sciences and by the Scientific Computing staff, Office of Energy Research, at the National Energy Research Supercomputer Center (Berkeley, CA).

References and Notes

(1) Impey, R. W.; Madden, P. A.; McDonald, I. R. *J. Phys. Chem.* **1983**, *87*, 5071.
(2) Nguyen, H. L.; Adelman, S. A. *J. Chem. Phys.* **1984**, *81*, 4564.
(3) Lee, S. H.; Rasaiah, J. C. *J. Chem. Phys.* **1994**, *101*, 6964.
(4) Lee, S. H.; Rasaiah, J. C. *J. Phys. Chem.* **1996**, *100*, 1420.
(5) Hynn, J. K.; Ichiye, T. *J. Phys. Chem.* **1997**, *101*, 3596.
(6) Mezei, M.; Beveridge, D. L. *J. Chem. Phys.* **1981**, *74*, 6902.
(7) Smith, D. E.; Dang, L. X. *J. Chem. Phys.* **1994**, *100*, 3757.
(8) Chandrasekhar, J.; Jorgensen, W. L. *J. Chem. Phys.* **1982**, *77*, 5080.
(9) Chandrasekhar, J.; Jorgensen, W. L.; Bigot, B. *J. Am. Chem. Soc.* **1982**, *104*, 4584. Sese, G.; Guardia, E.; *J. Phys. Chem.* **1995**, *99*, 12647; Madhusoodanan, M.; Tembe, B. L. *J. Phys. Chem.* **1995**, *99*, 44.
(10) Impey, R. W.; Sprik, M.; Klein, M. L. *J. Am. Chem. Soc.* **1987**, *109*, 5900. Rao, B. G.; Singh, U. C. *J. Am. Chem. Soc.* **1990**, *112*, 3803.
(11) Haag, W. R; Yao, C. C. D. *Environ. Sci. Technol.* **1992**, *26*, 1005. U.S. Department of Energy, Office of Environmental Management, FY 1995 Technology Development Needs Summary, 1994; pp 2−17.
(12) Koeing, K. E.; Lein, G. M.; Stucker, P; Kaneda, T.; Cram D. *J. Am. Chem. Soc.* **1979**, *101*, 3553.
(13) Chang, T.-M.; Dang, L. X.; Peterson, K. A. *J. Phys. Chem.* **1997**, *101*, 3413.
(14) Xantheas, S. S.; Dang, L. X. *J. Phys. Chem.* **1996**, *100*, 3989.
(15) Smith, D. E.; Dang, L. X. *J. Chem. Phys.* **1994**, *101*, 7873.
(16) Dang, L. X.; Garrett, B. C. *J. Chem. Phys.* **1993**, *99*, 2972.
(17) Ryckaert, J.; Ciccotti, G.; Berendsen, H. J. C. *J. Comput. Phys.* **1977**, *23*, 327.
(18) Chang, T.-M.; Peterson, K. A.; Dang, L. X. *J. Chem. Phys.* **1995**, *103*, 7502.
(19) Bopp, P. in *The Physics and Chemistry of Aqueous Ionic Solutions*; Bellissent-Funel, M. C., Neilson, G. W., Eds.; D. Reidel Publishing: Dordrecht, 1987; p 217.
(20) McQuarrie, D. A. *Statistical Mechanics*; Harper and Row: New York, 1976.
(21) Hubbard, J. *J. Chem. Phys.* **1978**, *68*, 1649.
(22) Impey, R. W.; Madden, P. A.; McDonald, I. R. *Mol. Phys.* **1982**, *46*, 513.